IAI Journals.ASM.org

Comparison of Models for Bubonic Plague Reveals Unique Pathogen Adaptations to the Dermis

Rodrigo J. Gonzalez,[a]* Eric H. Weening,[a] M. Chelsea Lane,[a]* Virginia L. Miller[a,b]

Department of Microbiology and Immunology, University of North Carolina, Chapel Hill, North Carolina, USA[a]; Department of Genetics, University of North Carolina, Chapel Hill, North Carolina, USA[b]

Vector-borne pathogens are inoculated in the skin of mammals, most likely in the dermis. Despite this, subcutaneous (s.c.) models of infection are broadly used in many fields, including *Yersinia pestis* pathogenesis. We expand on a previous report where we implemented intradermal (i.d.) inoculations to study bacterial dissemination during bubonic plague and compare this model with an s.c. model. We found that i.d. inoculations result in faster kinetics of infection and that bacterial dose influenced mouse survival after i.d. but not s.c. inoculation. Moreover, a deletion mutant of *rovA*, previously shown to be moderately attenuated in the s.c. model, was severely attenuated in the i.d. model. Lastly, based on previous observations where a population bottleneck from the skin to lymph nodes was observed after i.d., but not after s.c., inoculations, we used the latter model as a strategy to identify an additional bottleneck in bacterial dissemination from lymph nodes to the bloodstream. Our data indicate that the more biologically relevant i.d. model of bubonic plague differs significantly from the s.c. model in multiple aspects of infection. These findings reveal adaptations of *Y. pestis* to the dermis and how these adaptations can define the progression of disease. They also emphasize the importance of using a relevant route of infection when addressing host-pathogen interactions.

Host-pathogen interactions begin with transmission and continue as the pathogen disseminates into deeper tissues. These tissues are in themselves microenvironments with defined immunological characteristics and can serve as barriers to prevent spread. For arthropod-borne pathogens, the skin epithelium is the first barrier that must be surpassed to penetrate into deeper organs (1, 2). The complexity of the immune responses of each layer of the skin reflects the specificity at which this tissue can act upon invaders.

Based on its histological architecture, the skin can be divided into three main layers, namely, epidermis, dermis, and subcutaneous space (also known as hypodermis) (3). Each layer encompasses not only specific architectural qualities but also unique immunological characteristics that define them (2). How these characteristics influence the progression of infection is unknown. The epidermis is the outermost layer of the skin and constitutes a strong physical barrier that pathogens must cross to enter the body. Pathogens that survive in blood-feeding arthropods can cross this layer through the mechanical action of the arthropod's probing mouth parts (4). Consequently, the dermis, located immediately adjacent to the epidermis, is highly exposed to these pathogens. Because most arthropod vectors do not penetrate beyond the dermis to the subcutaneous (s.c.) space, the dermis is, most likely, the first tissue where initial host-pathogen interactions occur during vector-borne infections (1, 5–7).

Yersinia pestis is a Gram-negative bacterium and the causative agent of plague. This highly virulent pathogen was responsible for major pandemics in history and continues to survive in animal reservoirs in many parts of the world (8, 9). Bubonic plague is the most prevalent form of the disease and occurs after bacterial inoculation into the skin, typically by a flea vector (10). From the skin, *Y. pestis* disseminates to draining lymph nodes (LNs) via lymphatic vessels (11) and then to deeper organs through the bloodstream (12). Systemic dissemination results in septic shock, severe organ failure, and death.

Models of infection that target the s.c. space are broadly used in plague research (13–16) as this is a relatively easy tissue to target. However, the dermis is strongly implicated as the layer of the skin probed by fleas during transmission (5, 17). In comparison with s.c. models, intradermal (i.d.) inoculations require more dexterity and can be more challenging to implement in biosafety level three facilities, which are mandatory when handling fully virulent strains of *Y. pestis*. In this study, we further characterize the i.d. model we used in a previous study (11) and compare i.d. and s.c. inoculations to investigate whether infection model impacts progression of bubonic plague. We found substantial differences in disease progression after inoculation by the two different routes. In addition, we found that dissemination of bacteria from the LNs is restricted. These findings are relevant for the understanding of *Y. pestis* dissemination and pathogenesis and of host responses to different inoculation routes. Moreover, our study emphasizes the importance of using a biologically relevant model when studying host-pathogen interactions *in vivo*.

Received 6 February 2015 **Returned for modification** 26 March 2015
Accepted 21 April 2015

Accepted manuscript posted online 4 May 2015

Citation Gonzalez RJ, Weening EH, Lane MC, Miller VL. 2015. Comparison of models for bubonic plague reveals unique pathogen adaptations to the dermis. Infect Immun 83:2855–2861. doi:10.1128/IAI.00140-15.

Editor: A. Camilli

Address correspondence to Virginia L. Miller, vlmiller@med.unc.edu.

* Present address: Rodrigo J. Gonzalez, Department of Microbiology and Immunobiology, Harvard Medical School, Harvard University, Boston, Massachusetts, USA; M. Chelsea Lane, National Institutes of Health, Bethesda, Maryland, USA.

doi:10.1128/IAI.00140-15

MATERIALS AND METHODS

Bacterial cultures. Fully virulent *Y. pestis* CO92 was used in all the experiments of this study (18, 19). Bacteria were streaked on brain heart infusion (BHI; BD Biosciences, Bedford MA) agar plates from frozen stocks and incubated at 26°C for 48 h. Liquid cultures in BHI broth were incubated for 15 h at 26°C with aeration. The Δ*rovA* strain was constructed by allelic exchange, as described elsewhere (20). The Δ*psaA* strain was constructed using the λ Red recombination system, as described elsewhere (20, 21). The procedures employed to construct the isogenic set of 10 tagged strains used in the dissemination assays were previously described (11, 22). These 10 *Y. pestis* tagged strains have growth and virulence characteristics similar to those of untagged bacteria (11). For the dose-dependent survival assays (DDSA), an untagged wild-type (WT) strain was used.

Animal inoculations. Female C57BL/6J mice (6 to 8 weeks old; Jackson Laboratory, Bar Harbor, ME) were inoculated with *Y. pestis* after injection of a ketamine-xylazine mix. Intradermal (i.d.) inoculations were performed as previously described (11). Briefly, ~200 CFU in 2 μl was injected into the dorsal leaflet of the ear pinna with the aid of a Pump11 Elite syringe pump (Harvard Apparatus, Holliston, MA). The same procedure was used for the subcutaneous (s.c.) inoculations except that mice were injected in the ventral cervical region. Organs were harvested at different time points, homogenized, diluted, and plated on BHI agar to enumerate the bacteria in each organ. For the i.d. and s.c. inoculations, the superficial parotid LNs and the superficial cervical LNs, respectively, were harvested (23).

For the assay to determine the presence of a bottleneck, 9 of the 10 tagged strains were grown in BHI broth with 25 μg/ml kanamycin. The cultures were then mixed (equal optical density at 600 nm [OD_{600}] for each culture) and used to inoculate mice as previously described (11). For both routes (i.d. and s.c.), ~200 CFU of the mix was inoculated (~22 CFU of each of the nine tagged strains). The 10th tagged strain was omitted from the mix so it could be used as a negative control. Bacteria recovered from tissues were used for DNA extraction, this DNA was then used as a probe for Southern dot blot analysis, and results from the blots were scored as previously described (11). Statistical analysis was performed using a Mann-Whitney or Wilcoxon matched-pairs signed-rank test calculated by GraphPad Prism version 4.0c for Macintosh (GraphPad Software, La Jolla, CA). We established statistical significance at a P of <0.05.

This study was carried out in accordance with the *Guide for the Care and Use of Laboratory Animals* of the National Institutes of Health (24). All animal studies were approved by the Institutional Animal Care and Use Committee of the University of North Carolina at Chapel Hill (protocol 11-128). All efforts were made to minimize suffering; animals were monitored every 12 h following inoculation and were euthanized upon exhibiting signs of morbidity.

RESULTS

***Y. pestis* does not proliferate in the skin.** We previously used a murine i.d. model of infection in which the inoculum (~200 CFU) was injected in the dermis of the ear pinna (11). Because of the absence of subcutaneous tissue in the ear, this model results in i.d., as opposed to s.c., inoculation (25). A key attribute of our model is the use of a 2-μl inoculation volume, which contrasts with the 10-μl volume reported in previous studies using i.d. inoculation in the ear (25, 26). We considered that in comparison with larger volumes, the 2-μl model would mimic more closely the small volume that must be deposited by a flea during natural inoculations. In addition, the size of the injection wheal produced by a 10-μl volume in the skin is much larger than that produced by a 2-μl volume (Fig. 1A); we postulated that larger volumes could generate confounding effects due to tissue disruption. Thus, we established 2 μl as a preferred volume of inoculation. With this model, we noted that bacterial loads in the skin do not change significantly over time except when mice are subjected to neutrophil depletion (11). Because it has been reported that bacterial loads increase in the skin during *Y. pestis* infections (25, 26), we revisited our model to consider possible explanations for this discrepancy. Thus, we asked whether the inoculation volume affects bacterial proliferation in the skin. We compared bacterial loads in the skin after injection of the same bacterial dose using either 2 or 10 μl as the inoculation volume at a time point that precedes systemic dissemination (24 h postinoculation [hpi]). We found a small but significant increase in the number of CFU in the skin of mice injected with 10 μl in comparison with that in mice injected with 2 μl (Fig. 1B). This indicates that larger volumes of inoculation favor bacterial proliferation in the skin.

We also considered the possibility that the reported increase in bacterial numbers in the skin derives from measurements taken when the bacteria are circulating systemically (time points after 24 hpi). To test this, we inoculated mice in the right ear, and at 48 hpi, we determined the bacterial burdens in the left and right ears. The number of bacteria in the inoculated ear (right ear) was significantly larger than the ~200 CFU that was inoculated, which could

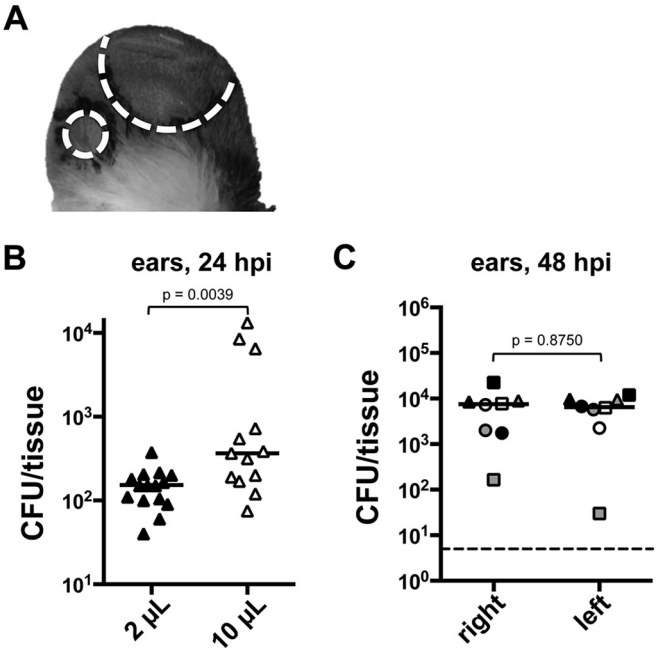

FIG 1 Bacterial proliferation in the dermis. (A) Mouse ear after injection of a volume of 2 μl (small circle) and 10 μl (large circle). The white dotted lines delineate the edges of the injection wheal (bubble). (B) Numbers of CFU in ears harvested at 24 hpi using a volume of 2 or 10 μl. The horizontal lines depict the median value of a group. All values were over the limit of detection. Spleens of these animals were negative (i.e., systemic spread had not occurred). Differences between groups were determined by a Mann-Whitney test, and the obtained P value is shown. (C) Numbers of CFU in right and left ears harvested at 48 hpi. Only the right ear was inoculated. Ears (left and right) represented with the same symbol (circle, triangle, or square) and color (black, gray, or white) belong to the same mouse, so a direct comparison between the inoculated and noninoculated ears can be appreciated. The horizontal lines depict the median value of a group. All values are over the limit of detection (dotted line). Differences between groups were determined by a Wilcoxon matched-pairs signed-rank test. For panels B and C, significance was established at a P of <0.05. Each symbol represents the number of CFU obtained from a tissue, and the dotted line shows the limit of detection. Data from two combined independent experiments are shown.

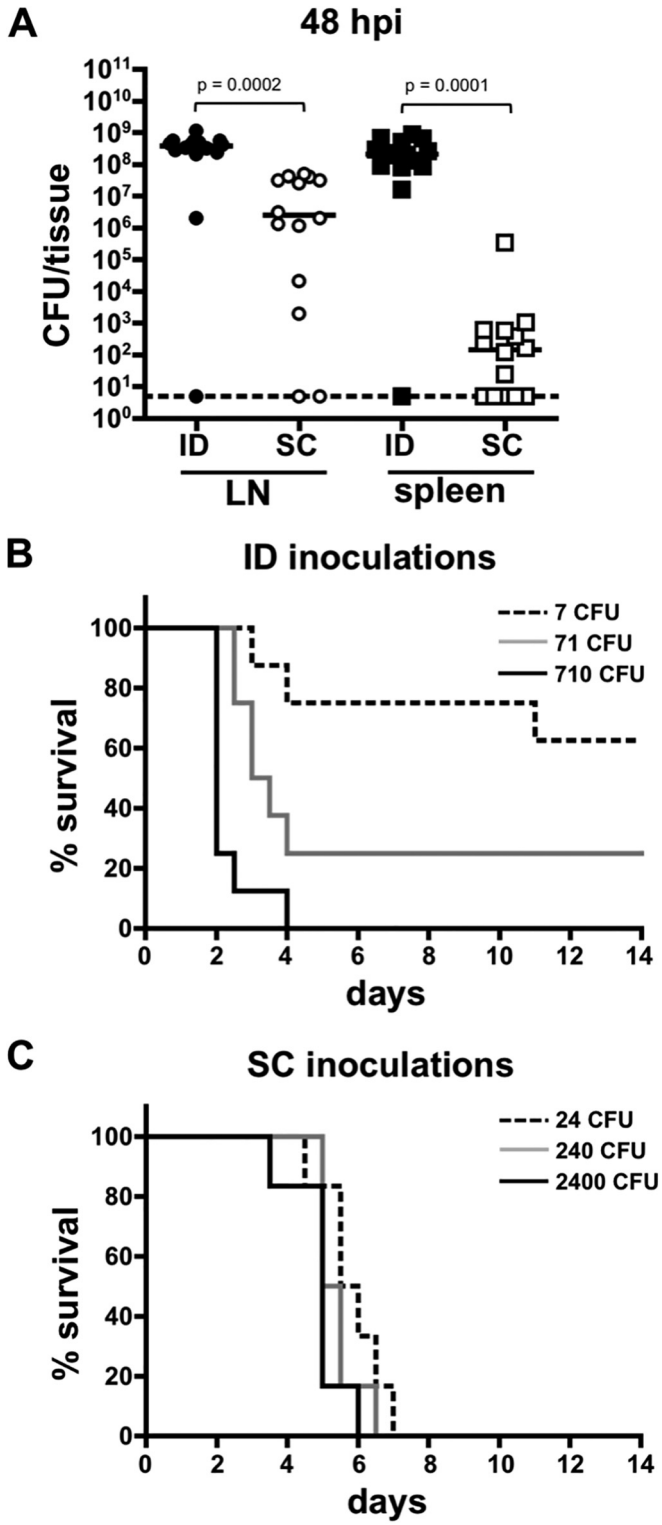

FIG 2 Kinetics of infection and survival in mice inoculated i.d. and s.c. (A) Numbers of CFU from LNs (circles) and spleens (squares) harvested 48 h after i.d. (black symbols) or s.c. (white symbols) inoculation. Each symbol represents the number of CFU obtained from a tissue. The horizontal lines depict the median value of a group. Differences between groups were determined by a Mann-Whitney test. Significance was established at a P of <0.05. The dotted line shows the limit of detection. Data from two combined independent experiments are shown. (B and C) DDSA of mice inoculated i.d. (B) or s.c. (C) using three different doses. Each line depicts the percentage of mice surviving in a group ($n = 8$ per inoculum for i.d., $n = 6$ per inoculum for s.c.) at different time points (in days). The dose for each group is shown in the upper right corner of each panel. Data from one representative experiment are shown.

be interpreted as *Y. pestis* proliferating in the skin. However, the bacterial loads in this ear were comparable to those in the uninoculated ear (left ear) (Fig. 1C). This suggests that large numbers of bacteria in the skin at later stages of infection derive from bacteria circulating systemically and not necessarily from net bacterial proliferation in this tissue. Of note, it is possible that inoculations with very high doses (>2,000 CFU) affect neutrophil activity (11) and result in bacterial proliferation. However, we think that these events are not relevant, as flea inoculations rarely result in high bacterial doses in the skin. Thus, overall, our data suggest that *Y. pestis* does not proliferate significantly in the dermis of the skin.

Intradermal inoculations result in faster kinetics but lower mortality rates than s.c. inoculations. We recently reported the presence of a bottleneck during i.d. inoculations and that the bottleneck was not observed when the bacteria were injected s.c. (11). With this important difference between the i.d. and s.c. models, we hypothesized that inoculations into these different layers of the skin could affect disease progression. To test this, mice were inoculated i.d. (ear, harvesting the parotid LN) or s.c. (scruff of the neck, harvesting the cervical LN), and bacterial loads in draining LNs and spleens at 48 hpi were determined (Fig. 2A). The median number of bacteria in LNs of mice inoculated i.d. was ~100-fold higher than the median value in LNs of mice inoculated s.c. This difference was determined to be statistically significant (Mann-Whitney test, $P = 0.0002$). Bacterial burdens in the spleen, an organ used to assess systemic dissemination, showed an even larger difference between groups. The median number of bacteria in spleens from mice inoculated i.d. was ~10^6-fold higher than in mice inoculated s.c. Faster kinetics of dissemination after i.d. injections do not derive from the anatomical localization of the draining LN, as the site of inoculation in the ear is considerably more distant to its draining LN than the site of inoculation in the neck, which is adjacent to the cervical draining LNs. These data indicate that the route of inoculation affects the kinetics of infection.

We had noted that when mice were inoculated i.d. with our normal dose (~200 CFU), approximately 1/10 of the animals did not have bacteria in the LNs (data not shown). These mice had the expected numbers of bacteria in the ear, confirming that they were inoculated properly. This suggests that the inoculation route could also impact mouse survival. A dose-dependent survival assay (DDSA) was used to determine differences in survival times for each of the inoculation routes. A DDSA can also reveal how these differences are influenced by the dose (number of CFU in the inocula). Mice were inoculated i.d. with a low (~7-CFU), medium (~71-CFU), or high (~710-CFU) dose, and survival was monitored during the following 14 days. Inoculation with the low dose resulted in 67% mouse survival (Fig. 2B). Survival rates of mice inoculated with the medium and high doses were 25% and 0%, respectively. For the whole group, death was first observed at day 2. Most mice died between days 2 and 4, with the exception of one mouse from the low-dose group, which died on day 11. For the group inoculated s.c., the doses used were ~24 CFU, ~240 CFU, and ~2,400 CFU. Regardless of the dose, no mice inoculated

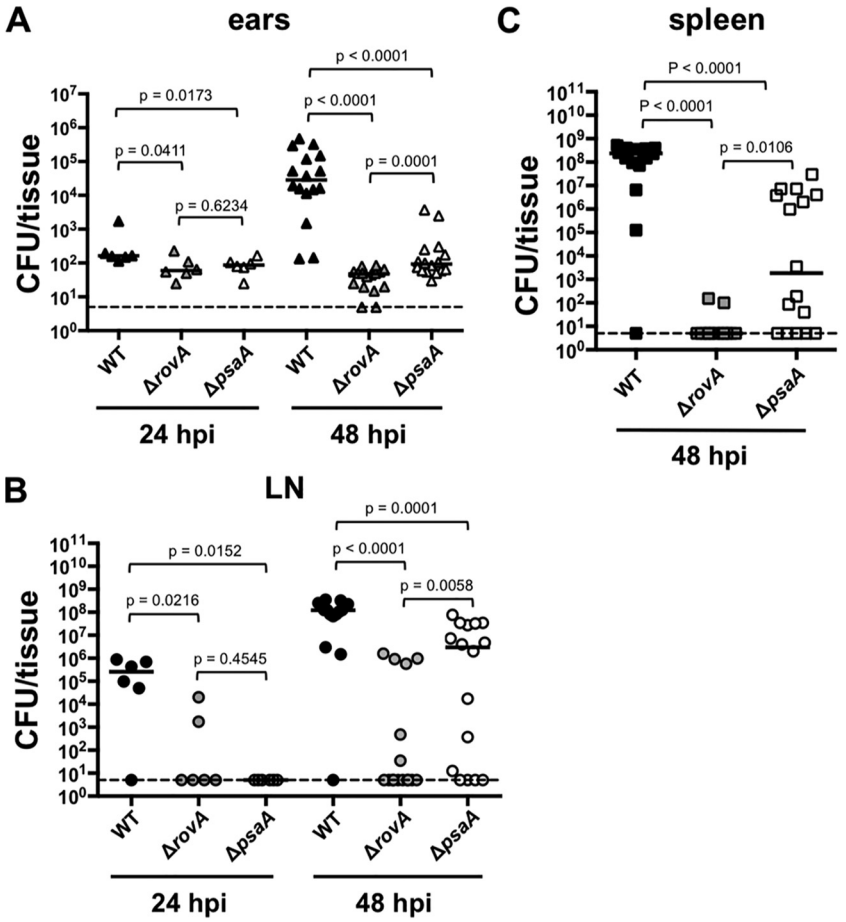

FIG 3 Kinetics of infection of Δ*rovA* and Δ*psaA* mutants after i.d. inoculation. Bacterial loads were determined in ears (A), LNs (B), and spleens (C) harvested at the indicated times after i.d. inoculation with ~200 CFU of WT (black), Δ*rovA* mutant (gray), or Δ*psaA* mutant (white) *Y. pestis*. Each symbol represents the number of CFU obtained from a tissue. The horizontal lines depict the median of the group. Differences between groups were determined by a Mann-Whitney test, and the obtained *P* value is shown. Data shown are from one experiment for the 24 hpi time point and from three combined independent experiments for the 48 hpi time point. Significance was established at a *P* of <0.05. The dotted line shows the limit of detection.

s.c. survived (Fig. 2C). With the exception of one mouse in the high-inoculum group that died at day 3.5, all mice died between days 4.5 and 7. These data indicate that mouse survival after i.d. inoculation, but not after s.c. inoculation, appeared to be linked to inoculum size.

A deletion mutant lacking a global regulator of *Y. pestis* is more attenuated after i.d. inoculation than after s.c. inoculation. We previously demonstrated that after s.c. inoculation, *Y. pestis* deletion mutants lacking the transcriptional regulator RovA or the putative antiphagocytic factor PsaA are attenuated (20, 27). Microarray and reverse transcription-quantitative PCR (qRT-PCR) analyses revealed that expression of *psaA* was substantially decreased in the Δ*rovA* strain. Because the degrees of attenuation of the two mutants were similar, we inferred that PsaA was the main (if not the only) virulence factor regulated by RovA during bubonic plague. Since we found important differences between our i.d. and s.c. models, we asked whether mutants characterized in the s.c. model would behave in the same way after i.d. inoculation. Thus, we tested the Δ*rovA* and Δ*psaA* strains in our i.d. model. We used time points relevant to the kinetics for this route (24 and 48 hpi), and in addition to LNs and spleens, we also harvested ears (site of inoculation). Both Δ*rovA* and Δ*psaA* strains were attenuated compared to WT *Y. pestis* (Fig. 3A, B, and C). At 24 hpi, the two mutant strains showed similar levels of attenuation in the ears and LNs when compared to one another. However, in contrast to what was observed in the s.c. model, the Δ*rovA* strain was significantly more attenuated than the Δ*psaA* strain at 48 hpi (Fig. 3). This difference was especially evident in LNs at 48 hpi (Fig. 3 B), where the median value of bacterial counts of the Δ*rovA* strain was at the limit of detection and the median number of CFU for the Δ*psaA* strain was 6 logs higher. Significant differences between the two strains were also observed in ears and spleens, although this most likely reflects delays in systemic infection by the Δ*rovA* strain that resulted from the lower levels of LN colonization by this mutant (Fig. 3A and C). Overall, this indicates that after i.d. inoculation, *Y. pestis* lacking *rovA* is significantly more attenuated than *Y. pestis* lacking *psaA*. This finding differs from what was observed after s.c. inoculations, in which case both mutants were equally attenuated (20).

An s.c. route of inoculation reveals a bottleneck in bacterial dissemination from LNs to deeper organs. Using oligonucleotide-tagged isogenic strains of *Y. pestis*, we previously identified a bottleneck during early stages of infection following i.d. inoculation (11); only a small fraction of the tagged strains that were

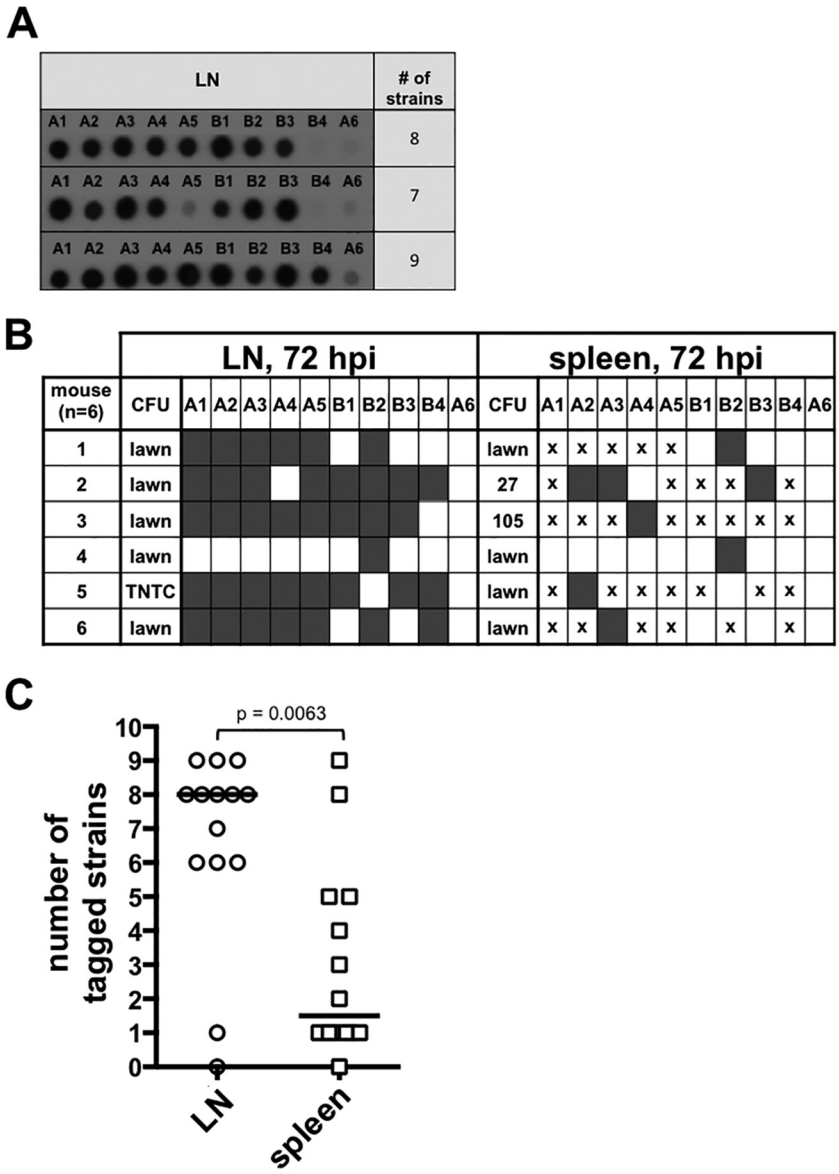

FIG 4 Bottleneck from LNs to spleen revealed after s.c. inoculation. (A) Southern dot blot of bacterial DNA obtained from the LNs of mice inoculated s.c. with nine oligonucleotide-tagged strains of *Y. pestis*. LNs were harvested at 48 hpi. Each row depicts the results for a single mouse. Each strain is identified (A1 to A5 and B1 to B4; A6 was used as a negative control). (B) Comparison of tagged strains present in LNs and spleens at 72 h after s.c. inoculations. Each row depicts the results from a single mouse (six mice used). The number of CFU obtained from a tissue and from which DNA was extracted is also shown. Plates that were completely covered with a layer of bacteria (as opposed to isolated colonies) are identified as "lawn." Plates with isolated colonies that were too numerous to count are identified as "TNTC." Tagged strains in each organ are shown as present (gray) or absent (white). The "X" symbol represents tagged strains present in LNs that are absent in spleens. For panels A and B, results from one representative experiment are shown. (C) Quantification of tagged strains present in LNs and spleens at 48 h after s.c. inoculation. Each symbol represents the number of tags obtained from a tissue. Horizontal lines represent the median of the group. Statistically significant differences between groups were determined by a Mann-Whitney test establishing significance at a P of <0.05.

inoculated i.d. into the skin were subsequently present in draining LNs. This suggested that the bottleneck affected bacterial dissemination from the skin to the LNs. We suspected that a second bottleneck existed in the dissemination of *Y. pestis* from the LNs to systemic sites, because in some instances a tagged strain that was present in the LNs was absent in the spleen. However, this was difficult to test because the number of tagged strains in the LNs after i.d. inoculations is very low. Thus, it is impossible to assess any further reduction in the numbers of tagged strains beyond the LNs. Notably, in the same study, we found that the bottleneck was almost completely abrogated when *Y. pestis* was inoculated s.c., as nearly all tagged strains were found in draining LNs (Fig. 4A). Therefore, we used this model as a strategy to test whether *Y. pestis* passes through a bottleneck when disseminating from LNs to systemic circulation. We assumed that the route of inoculation affects only dissemination from the skin to the LNs and does not affect dissemination beyond this compartment. Mice were inoculated s.c. with nine tagged strains, and LNs and spleens were harvested at 72 hpi, a time point when the numbers of CFU in the spleens are close to maximal. Five out of six mice had fewer tagged

strains in the spleens than in the LNs (Fig. 4B). The number of tagged strains present in the LNs but absent in the spleens ranged from five to eight. Differences between the numbers of tagged strains in LNs and spleens were significant (Fig. 4C). These data indicate that only a few of the tagged strains in the LNs predominate in a systemic organ (spleen).

DISCUSSION

Only in recent years have we begun to appreciate the significance of the differences between *in vivo* and *in vitro* approaches to studying host-pathogen interactions. This has resulted in the development of new animal models with a goal of mimicking natural infections as closely as possible. However, a major limitation of implementing animal models is how little is known about what aspects of a natural infection truly affect disease progression. In this study, we report important differences in the progression of bubonic plague in a comparison of the more commonly used s.c. route and the more biologically relevant i.d. route.

We observed that bacteria are able to colonize the host more rapidly (i.e., faster kinetics) after i.d. than after s.c. inoculations. This might be due to differences in the density and the anatomy of lymphatic vessels in each layer of the skin. The dermis is rich in terminal lymphatic vessels, which are absent in the epidermis and the s.c. space (28). Terminal lymphatic vessels lack smooth muscle cells and a basal membrane. The absence of these two elements increases the permeability of the vessels and makes them able to readily take up lymph and antigen (29). This is exemplified by experiments in which dyes to map lymphatic vessels for tumor detection are detected faster in LNs after i.d. injection than in LNs after s.c. injection (30). Unlike terminal lymphatic vessels, collecting lymphatics possess circumferential smooth muscle cells, are surrounded by a basement membrane, and are found in the s.c. layer of the skin (29). The presence of smooth muscle cells and a basement membrane restricts the access of particles into the lumen of the lymphatic vessels and makes them less efficient in antigen uptake. In addition to lymphatic vessel physiology, it also has been suggested that the dermis is subject to high fluid pressures (28). High pressures are important to drain fluid from the dermis to prevent edema and could also contribute to more efficient movement of *Y. pestis* to the LNs. This is especially true if, as we have previously suggested, *Y. pestis* travels to LNs freely with the flow of lymph (11). Thus, this suggests that *Y. pestis* cannot access LNs through lymphatic vessels as easily when deposited in the s.c. space as when deposited into the dermis.

Intriguingly, we found that while the kinetics of infection are faster when *Y. pestis* is delivered into the dermis, some mice survive after i.d. inoculation but none after s.c. inoculation. This is most evident when low inocula are used. Most mice survived after inoculation of 7 CFU in the dermis and none after inoculation of a very similar dose (24 CFU) in the s.c. space. In our bottleneck study, we found that a small percentage of i.d. inoculated mice did not have any detectable bacteria in their LNs and spleens (11). This suggested that the bottleneck could be highly efficient. It would be expected that the effects of a barrier (i.e., bottleneck) that limits dissemination to LNs are stronger when few bacteria are inoculated and weaker when larger numbers of bacteria are used. Consequently, all mice inoculated i.d. with a high inoculum (~710 CFU) died, and most of the mice inoculated with a low inoculum (~7 CFU) survived. Unlike the dermis, the s.c. layer of the skin possesses a very limited number of resident cells of the immune response (31). In addition, the s.c. space is less vascularized than the dermis, and, thus, access to it by infiltrating immune cells might be less efficient (3, 31). We speculate that a less efficient immune response could allow for local bacterial replication in the s.c. space favoring subsequent dissemination that is not influenced by an initial low dose.

The use of the i.d. model also demonstrated a more pronounced attenuation of the Δ*rovA* mutant than previously observed using the s.c. model (20). We speculate that this indicates a role for RovA-regulated genes in bacterial adaptation to the immune response of the dermis. While many aspects of the anatomy and physiology of the different layers of the skin are understood, their effects on the immune response to pathogens are not clear. However, studies in the cancer and vaccine development fields have shed some light on the effects of the immune responses of the different layers of the skin. Bonnotte and collaborators found that injection of a tumorigenic cell line results in tumor formation after s.c. but not i.d. injection in rats (32). In another study, injection of a virus-like particle to test its immunogenicity showed more LN involvement and cellular response after i.d. injection than with s.c. delivery (33). In addition, results favoring the use of i.d. over s.c. inoculations have been reported in experiments using an HIV-1 antigen in vaccine development against this virus (34). Much less work has been done comparing routes of inoculation during cutaneous infections caused by vector-borne pathogens. One exception is the work done with *Leishmania* parasites in which the use of an i.d. route appeared to recreate disease progression more accurately than an s.c. route (7). Together these studies indicate that the different layers of the skin differ considerably in the immune responses they can elicit. Differences in the immune response might account for the different phenotypes that the Δ*rovA* strain shows after inoculation in each layer of the skin. Thus, in the s.c. space, RovA seems to be primarily important as a regulator of a single locus (*psa*). In contrast, in the dermis, the more severe attenuation of the Δ*rovA* strain suggests that RovA regulates additional genes that play a relevant role during infection. Our experiments highlight the importance of using a biologically relevant model when determining the levels of attenuation of deletion mutants.

Lastly, while we support the use of an i.d. model of infection, we think s.c. inoculations can be useful as an experimental strategy to answer some questions regarding bacterium-host interactions. For example, we used the s.c. model as an experimental strategy to test for the reduction of tagged strains during late stages of infection (dissemination from LNs to systemic sites). This reduction had already been observed in the i.d. route, but quantification was challenging. The s.c. inoculation route resulted in enough tagged strains in the LNs to determine whether any of them were lost as disease progressed to a systemic organ. With this strategy, we confirmed that only a fraction of the tagged strains present in the LNs predominate in the spleen. This is in agreement with our definition of a bottleneck. While the exact location of this bottleneck is unknown, we think it might result from as yet uncovered immune processes in the LNs or blood.

For vector-borne infections, including bubonic plague, well-established models might need to be revisited and modifications to these models might need to be considered to optimize our ability to make biologically relevant observations. As we established, in addition to being more biologically relevant, the observations made using these approaches differ considerably from those obtained by more

conventional alternatives. Overall, we propose that approaches that use i.d. inoculations (along with fully virulent strains) should be given priority when studying the pathogenesis of *Y. pestis*.

ACKNOWLEDGMENTS

This work was supported by grants R21AI105271 and U54AI057157 (Southeast Regional Center for Biodefense and Emerging Infectious Diseases, project 006) from NIH to V.L.M. and the Robert D. Watkins Fellowship from the American Society for Microbiology to R.J.G. This research was conducted while M. Chelsea Lane was a postdoctoral fellow at the University of North Carolina, Chapel Hill.

We thank Kim Walker for valuable assistance in critically reviewing the manuscript.

REFERENCES

1. **Chong SZ, Evrard M, Ng LG.** 2013. Lights, camera, and action: vertebrate skin sets the stage for immune cell interaction with arthropod-vectored pathogens. Front Immunol **4:**286. http://dx.doi.org/10.3389/fimmu.2013.00286.
2. **Nestle FO, Di Meglio P, Qin J-Z, Nickoloff BJ.** 2009. Skin immune sentinels in health and disease. Nat Rev Immunol **9:**679–691. http://dx.doi.org/10.1038/nri2622.
3. **Teunissen MBM, Haniffa M, Collin MP.** 2012. Insight into the immunobiology of human skin and functional specialization of skin dendritic cell subsets to innovate intradermal vaccination design. Curr Top Microbiol Immunol **351:**25–76. http://dx.doi.org/10.1007/82_2011_169.
4. **Frischknecht F.** 2007. The skin as interface in the transmission of arthropod-borne pathogens. Cell Microbiol **9:**1630–1640. http://dx.doi.org/10.1111/j.1462-5822.2007.00955.x.
5. **Sebbane F, Jarrett CO, Gardner D, Long D, Hinnebusch BJ.** 2006. Role of the *Yersinia pestis* plasminogen activator in the incidence of distinct septicemic and bubonic forms of flea-borne plague. Proc Natl Acad Sci U S A **103:**5526–5530. http://dx.doi.org/10.1073/pnas.0509544103.
6. **Choumet V, Attout T, Chartier L, Khun H, Sautereau J, Robbe-Vincent A, Brey P, Huerre M, Bain O.** 2012. Visualizing non infectious and infectious *Anopheles gambiae* blood feedings in naive and saliva-immunized mice. PLoS One **7:**e50464. http://dx.doi.org/10.1371/journal.pone.0050464.
7. **Belkaid Y, Kamhawi S, Modi G, Valenzuela J, Noben-Trauth N, Rowton E, Ribeiro J, Sacks DL.** 1998. Development of a natural model of cutaneous leishmaniasis: powerful effects of vector saliva and saliva preexposure on the long-term outcome of *Leishmania major* infection in the mouse ear dermis. J Exp Med **188:**1941–1953. http://dx.doi.org/10.1084/jem.188.10.1941.
8. **Bos KI, Schuenemann VJ, Golding GB, Burbano HA, Waglechner N, Coombes BK, McPhee JB, DeWitte SN, Meyer M, Schmedes S, Wood J, Earn DJD, Herring DA, Bauer P, Poinar HN, Krause J.** 2011. A draft genome of *Yersinia pestis* from victims of the Black Death. Nature **478:**506–510. http://dx.doi.org/10.1038/nature10549.
9. **Butler T.** 2013. Plague gives surprises in the first decade of the 21st century in the United States and worldwide. Am J Trop Med Hyg **89:**788–793. http://dx.doi.org/10.4269/ajtmh.13-0191.
10. **Wimsatt J, Biggins DE.** 2009. A review of plague persistence with special emphasis on fleas. J Vector Borne Dis **46:**85–99.
11. **Gonzalez RJ, Lane MC, Wagner NJ, Weening EH, Miller VL.** 2015. Dissemination of a highly virulent pathogen: tracking the early events that define infection. PLoS Pathog **11:**e1004587. http://dx.doi.org/10.1371/journal.ppat.1004587.
12. **Sebbane F, Gardner D, Long D, Gowen BB, Hinnebusch BJ.** 2005. Kinetics of disease progression and host response in a rat model of bubonic plague. Am J Pathol **166:**1427–1439. http://dx.doi.org/10.1016/S0002-9440(10)62360-7.
13. **Demeure CE, Blanchet C, Fitting C, Fayolle C, Khun H, Szatanik M, Milon G, Panthier J-J, Jaubert J, Montagutelli X, Huerre M, Cavaillon J-M, Carniel E.** 2012. Early systemic bacterial dissemination and a rapid innate immune response characterize genetic resistance to plague of SEG mice. J Infect Dis **205:**134–143. http://dx.doi.org/10.1093/infdis/jir696.
14. **Lenz JD, Lawrenz MB, Cotter DG, Lane MC, Gonzalez RJ, Palacios M, Miller VL.** 2011. Expression during host infection and localization of *Yersinia pestis* autotransporter proteins. J Bacteriol **193:**5936–5949. http://dx.doi.org/10.1128/JB.05877-11.
15. **Abu Khweek A, Fetherston JD, Perry RD.** 2010. Analysis of HmsH and its role in plague biofilm formation. Microbiology **156:**1424–1438. http://dx.doi.org/10.1099/mic.0.036640-0.
16. **Oyston PC, Dorrell N, Williams K, Li SR, Green M, Titball RW, Wren BW.** 2000. The response regulator PhoP is important for survival under conditions of macrophage-induced stress and virulence in *Yersinia pestis*. Infect Immun **68:**3419–3425. http://dx.doi.org/10.1128/IAI.68.6.3419-3425.2000.
17. **Hinnebusch BJ.** 2005. The evolution of flea-borne transmission in *Yersinia pestis*. Curr Issues Mol Biol **7:**197–212.
18. **Parkhill J, Wren BW, Thomson NR, Titball RW, Holden MT, Prentice MB, Sebaihia M, James KD, Churcher C, Mungall KL, Baker S, Basham D, Bentley SD, Brooks K, Cerdeño-Tárraga AM, Chillingworth T, Cronin A, Davies RM, Davis P, Dougan G, Feltwell T, Hamlin N, Holroyd S, Jagels K, Karlyshev AV, Leather S, Moule S, Oyston PC, Quail M, Rutherford K, Simmonds M, Skelton J, Stevens K, Whitehead S, Barrell BG.** 2001. Genome sequence of *Yersinia pestis*, the causative agent of plague. Nature **413:**523–527. http://dx.doi.org/10.1038/35097083.
19. **Doll JM, Zeitz PS, Ettestad P, Bucholtz AL, Davis T, Gage K.** 1994. Cat-transmitted fatal pneumonic plague in a person who traveled from Colorado to Arizona. Am J Trop Med Hyg **51:**109–114.
20. **Cathelyn JS, Crosby SD, Lathem WW, Goldman WE, Miller VL.** 2006. RovA, a global regulator of *Yersinia pestis*, specifically required for bubonic plague. Proc Natl Acad Sci U S A **103:**13514–13519. http://dx.doi.org/10.1073/pnas.0603456103.
21. **Datsenko KA, Wanner BL.** 2000. One-step inactivation of chromosomal genes in *Escherichia coli* K-12 using PCR products. Proc Natl Acad Sci U S A **97:**6640–6645. http://dx.doi.org/10.1073/pnas.120163297.
22. **Walters MS, Lane MC, Vigil PD, Smith SN, Walk ST, Mobley HLT.** 2012. Kinetics of uropathogenic *Escherichia coli* metapopulation movement during urinary tract infection. mBio **3**(1):e00303-11. http://dx.doi.org/10.1128/mBio.00303-11.
23. **Van den Broeck W, Derore A, Simoens P.** 2006. Anatomy and nomenclature of murine lymph nodes: descriptive study and nomenclatory standardization in BALB/cAnNCrl mice. J Immunol Methods **312:**12–19. http://dx.doi.org/10.1016/j.jim.2006.01.022.
24. **National Research Council.** 2011. Guide for the care and use of laboratory animals, 8th ed. National Academies Press, Washington, DC.
25. **Guinet F, Carniel E.** 2003. A technique of intradermal injection of *Yersinia* to study *Y. pestis* physiopathology. Adv Exp Med Biol **529:**73–78.
26. **Bosio CF, Jarrett CO, Gardner D, Hinnebusch BJ.** 2012. Kinetics of innate immune response to *Yersinia pestis* after intradermal infection in a mouse model. Infect Immun **80:**4034–4045. http://dx.doi.org/10.1128/IAI.00606-12.
27. **Weening EH, Cathelyn JS, Kaufman G, Lawrenz MB, Price P, Goldman WE, Miller VL.** 2011. The dependence of the *Yersinia pestis* capsule on pathogenesis is influenced by the mouse background. Infect Immun **79:**644–652. http://dx.doi.org/10.1128/IAI.00981-10.
28. **O'Mahony S, Rose SL, Chilvers AJ, Ballinger JR, Solanki CK, Barber RW, Mortimer PS, Purushotham AD, Peters AM.** 2004. Finding an optimal method for imaging lymphatic vessels of the upper limb. Eur J Nucl Med Mol Imaging **31:**555–563. http://dx.doi.org/10.1007/s00259-003-1399-3.
29. **Shayan R, Achen MG, Stacker SA.** 2006. Lymphatic vessels in cancer metastasis: bridging the gaps. Carcinogenesis **27:**1729–1738. http://dx.doi.org/10.1093/carcin/bgl031.
30. **Kersey TW, Van Eyk J, Lannin DR, Chua AN, Tafra L.** 2001. Comparison of intradermal and subcutaneous injections in lymphatic mapping. J Surg Res **96:**255–259. http://dx.doi.org/10.1006/jsre.2000.6075.
31. **Combadiere B, Liard C.** 2011. Transcutaneous and intradermal vaccination. Hum Vaccin **7:**811–827. http://dx.doi.org/10.4161/hv.7.8.16274.
32. **Bonnotte B, Gough M, Phan V, Ahmed A, Chong H, Martin F, Vile RG.** 2003. Intradermal injection, as opposed to subcutaneous injection, enhances immunogenicity and suppresses tumorigenicity of tumor cells. Cancer Res **63:**2145–2149.
33. **Cubas R, Zhang S, Kwon S, Sevick-Muraca EM, Li M, Chen C, Yao Q.** 2009. Virus-like particle (VLP) lymphatic trafficking and immune response generation after immunization by different routes. J Immunother **32:**118–128. http://dx.doi.org/10.1097/CJI.0b013e31818f13c4.
34. **Liard C, Munier S, Arias M, Joulin-Giet A, Bonduelle O, Duffy D, Shattock RJ, Verrier B, Combadiere B.** 2011. Targeting of HIV-p24 particle-based vaccine into differential skin layers induces distinct arms of the immune responses. Vaccine **29:**6379–6391. http://dx.doi.org/10.1016/j.vaccine.2011.04.080.